

Received 12 July 2018; revised 31 August 2018; accepted 1 September 2018. Date of publication 17 September 2018; date of current version 1 October 2018.
The review of this paper was arranged by Editor C. C. McAndrew.

Digital Object Identifier 10.1109/JEDS.2018.2868686

Consideration of UFET Architecture for the 5 nm Node and Beyond Logic Transistor

UTTAM KUMAR DAS¹ (Student Member, IEEE), GEERT ENEMAN², RAVI SHANKAR R. VELAMPATI³,
YOGESH SINGH CHAUHAN⁴ (Senior Member, IEEE), K. B. JINESH⁵, AND TARUN K. BHATTACHARYYA¹

¹ Department of Electronics and Electrical Communication Engineering, Indian Institute of Technology Kharagpur, Kharagpur 721302, India

² TCAD Group, imec, 3001 Leuven, Belgium

³ VLSI Fabrication Division, Semiconductor Laboratory, Chandigarh 160071, India

⁴ Department of Electrical Engineering, Indian Institute of Technology Kanpur, Kanpur 208016, India

⁵ Department of Physics, Indian Institute of Space Science and Technology, Trivandrum 695547, India

CORRESPONDING AUTHOR: U. K. DAS (e-mail: uttamec.jgec@gmail.com)

This work was supported in part by the Department of Space, Govt. of India, and in part by the Department of Science and Technology, Govt. of India. This paper is an extension version of the paper entitled "Consideration of UFET architecture for the 5nm node and beyond logic transistor" accepted in IEEE Silicon Nanoelectronics Workshop 2018 (SNW2018).

ABSTRACT In this paper, we propose a trench MOS architecture for the upcoming 5 nm node and beyond logic transistor. The intended device has a gate formed vertically downward, with added spacers along the gate to S/D sidewall. In doing so, the recessed device having longer channel length (than the defined gate footprint) would be a constructive approach to limit the short channel effects (SCE). The novel transistor has the potential to enable the scaling of gate length (footprint) less than 10 nm and contacted gate pitch below 32 nm, resulting in the smallest active area (on-wafer footprint) for a single device. Novel process steps are simulated depicting easier fabrication while the electrical analysis shows a better electrostatic control over any unwanted leakage flows. Along with the area scaling and SCE control, the planar upper surface allows a vertical integration. Growing another flipped device on top surface permits the designer to implement a logic circuit on a footprint of a single device, achieving ~50% area gain further. TCAD based simulations were performed to design and characterize the performances of an individual device and the vertical inverter.

INDEX TERMS CMOS Logic, 5 nm Node, GAA-NWFET, UFET, 3D Integration, TCAD.

I. INTRODUCTION

Size of the silicon transistor is continuously scaled in every generation to deliver the smaller and faster electronics technology [1]. Since last few decades, the trend of CMOS scaling was accelerated by many prime movers such as strained silicon and high-k/metal-gate technology [2]–[4]. However, while scaling down below 32 nm node, short channel effects (SCE), such as sub-threshold leakage become a major concern in planar MOS devices. Therefore, the planar MOSFET was replaced by a tri-gate architecture (FinFET) to improve the electrostatic control at the 22nm node [5]. Subsequently, the major industries followed the same FinFET based architecture for their 16/14nm, 10nm and 7nm node (N7) technology [6]–[11]. Aiming at the forthcoming sub-7nm node CMOS device, the critical key dimensions are predicted in Table-1. The expected contacted

gate pitch (CGP) would be below 32nm for beyond 5nm node technology. This tighter CGP budgeting would lead the gate length scaling of less than 10nm. Even though the FinFET has gate wrapping around the channel providing better electrostatics, yet controlling the short channel effects at this shortest gate length would be a real big challenge.

Researchers are looking into Gate-All-Around (GAA) architectures, such as Nanowire (NW) /NanoSheet (NS) as the leading device structure for the 5nm node due to its superior electrostatics integrity than the FinFET [12], [13]. Although the NW with reduced diameter delivers best electrostatic control, the reduction of channel area reduces the current driving capability significantly. However, compromising electrostatics to some extent in GAA-NS device, drive currents are improved, yet the tighter constraint on width scaling doesn't allow a designer to scale down device

TABLE 1. Node to Node Scaling Target.

Technology Node	N7	N5	N3
Contacted Gate Pitch (CGP) (nm)	42	32	24
Metal Pitch(MP) (nm)	32	24	18
Gate Length (L_g) (nm)	14	10	6

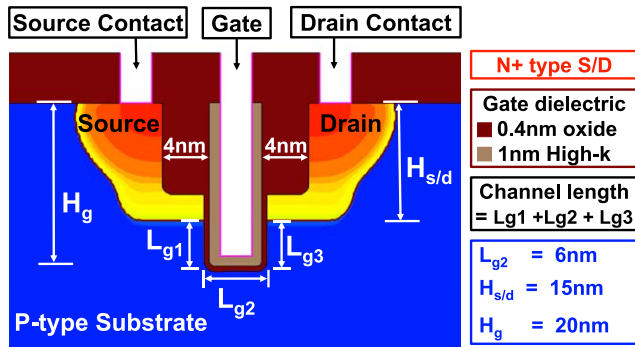


FIGURE 1. Cross-sectional view of the proposed UFET transistor having foot-print gate length of 6nm and trench depth of 20 nm.

size further. Though drive current in GAA devices can be increased by stacking multiple wires/sheets per fin, but a taller fin device increases the process complexity and parasitic capacitances [14], [15].

In this study, an alternative device structure, a vertically integrated recessed channel transistor [16], with parasitic modifications is proposed as an alternative approach to continue the CMOS scaling. The cross-sectional view of the proposed nano-scale transistor is shown in Fig. 1. As the channel forms a U-shape inside the bulk, we referred this transistor as UFET.

Though recessed channel devices are already being used in DRAM cell [17], [18], and the U-shaped FET (V-shaped FET) are also being used in power semiconductor applications since last few decades [19]. We have studied the recessed channel planar device targeting the upcoming 5nm node and beyond logic technologies.

TCAD Sprocess [20] was used to implement the individual device structures and Sdevice [21] simulation with SRH, auger, BTBT recombination, bandgap narrowing, anisotropic density gradient, fixed interface charge, mobility model with multivalley correction, thin inversion layer correction with high-k dielectric, and quantum correction for the inversion layer were used to obtain electrical performances for both UFET and GAA-NW. Mixed-mode simulation was performed to obtain the characteristics of a vertically integrated inverter device.

II. DEVICE SPECIFICATION AND PROCESS FLOW

The n-channel UFET transistor was built on a p-type bulk Si substrate considering the surface on {100} plane and sidewall surfaces along with the {110} plane. The source and drain regions were doped with n+ type active dopant atoms. The gate trench was considered of length 6nm and

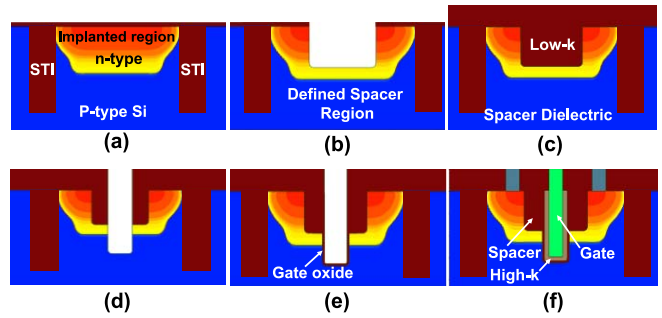


FIGURE 2. Novel process steps followed to make the UFET device.

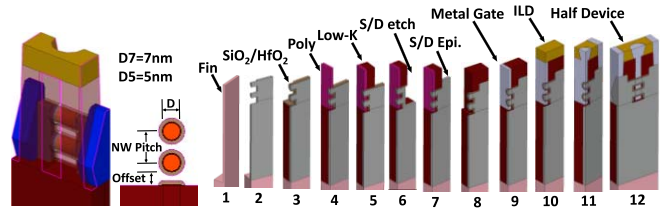


FIGURE 3. Process flow used to create two stacked GAA-NW transistor with epitaxial S/D contacts.

depth 20nm. The gate dielectric of 0.4nm oxide (SiO_2) and 1nm high-k (HfO_2) were used. The recessed gate was filled with the metal line considering proper work-function (WF). Gate to S/D spacers (low-k) were considered having a height of 6nm and length of 4nm. Silicide contacts similar to a planar MOSFET [4] were made at top of the source and drain regions which may provide a benefit of reducing the increased contact resistivity over epitaxial or wrap around contacts in GAA architecture. In this device, actual channel length would be the sum of $L_{g1} + L_{g2} + L_{g3}$. Other parameters of the n-channel UFET device are specified in Table 2.

TABLE 2. Specifications for n-Channel UFET Device.

Parameters	Value	Unit
S/D doping (N_d)	3×10^{20}	/cm ³
Channel doping (N_a)	2×10^{17}	/cm ³
Effective oxide thickness (EOT)	0.577	nm
Drive Voltage (V_{dd})	0.6	V
Targeted off state current (I_{off_target})	10×10^{-9}	A/ μm

The recent development of advanced patterning techniques (EUV) has enabled the most critical process steps [22]. The novel process steps to fabricate the n-channel UFET device is described in Fig. 2. The p-type silicon substrate was patterned and implanted to define the active region (source, gate and drain region together) leading to the high-temperature activation at beginning of the process. Then, the center region of doped silicon was patterned and etched away for the S/D to gate spacers as shown in Fig. 2(b). Subsequently, the spacer material (low-k) was filled into the trench to minimize the S/D to gate overlap parasitic

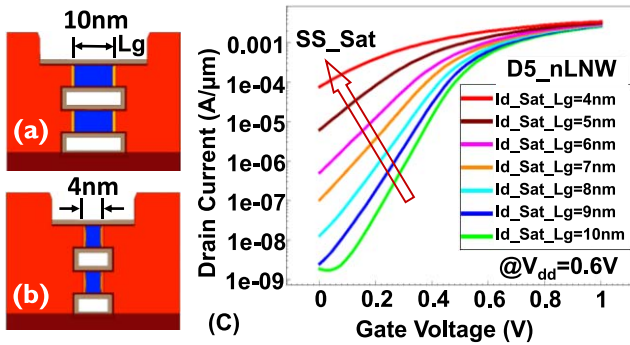


FIGURE 4. Deviation of sub-threshold currents while scaling the gate length from 10nm to 4nm for 5nm diameter (D5) based GAA-NW.

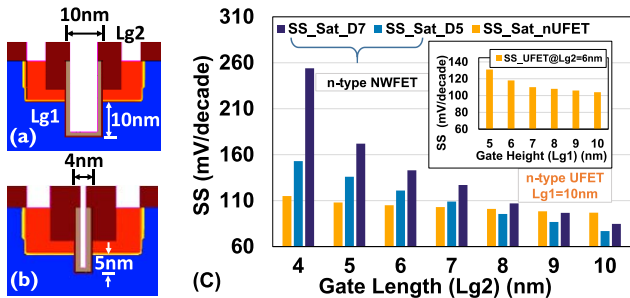


FIGURE 5. Comparisons of the Sub-threshold Slope (SS) of UFET and D7/D5 GAA-NW.

capacitance, as shown in Fig. 2(c). A narrow trench was then created by selectively removing the spacer dielectric and silicon underneath to open the gate region as shown in Fig. 2(d). After that, a thin conformal oxide covering was grown up for interface oxide layer. Finally, a high-k layer deposition followed by trench fill up with the gate material was performed. Narrow windows were created to make the contacts for source and drain terminal. The complete device is shown in Fig. 2(f). Similarly, the p-channel UFET transistor can be designed and processed on an n-type silicon substrate. In Fig. 3, we show the steps used of making GAA-NW device [23] with specifications similar to [15].

III. ELECTRICAL PERFORMANCES OF UFET AND GAA-NW

While scaling down below 10nm gate length (Lg), a stronger gate control is merely achieved by a thinner diameter for GAA-NW's. Above all, at this dimension ballistic [24] flow is enabled significantly. In the UFET channel, the straight lines are also within 5nm to 10nm, so the Lg1, Lg2 and Lg3 region might experience more ballistic conduction compared to the two corner regions, however, at corners the carrier will face more scattering as well as change the path direction leading to a more drift-diffusion conduction. Hence, more extensive studies are required to benchmark the ON state drive current in both the devices. At this point, a drift-diffusion based simulation model was used to analyze the sub-threshold characteristics. The obtained total current was normalized (by the width of UFET (W = 18nm) and the fin

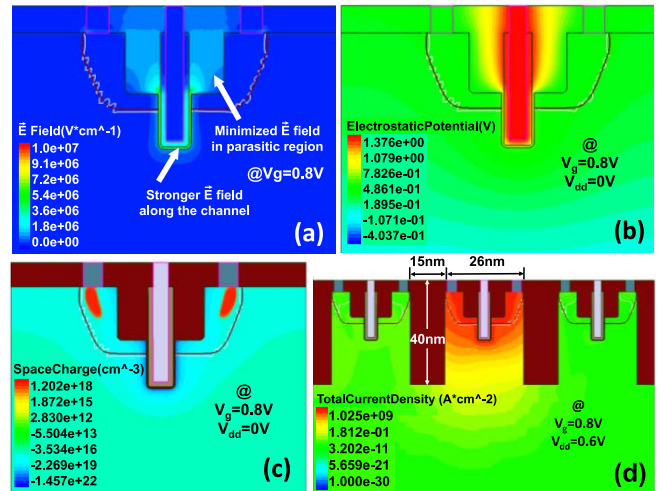


FIGURE 6. The electrical behavior in UFET: (a) Electric field distribution, (b) Spreading of Electrostatics potential, (c) Space Charges, and (d) STI isolation.

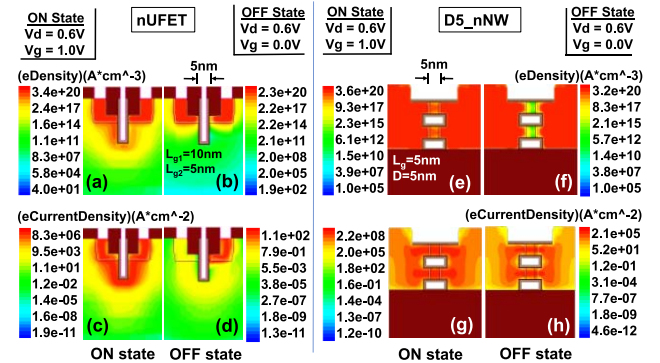


FIGURE 7. Carrier (electron) distributions in both the UFET and GAA-NW devices at a gate length of 5nm (footprint).

pitch of NW (FP = 18nm) and targeted at the same off-state current (10nA/μm).

Fig. 4(a) and 4(b) predicts gate length scaling of two stacked GAA-NW considering 5nm wire diameter (D5). Fig. 4(c) shows the degradation of sub-threshold slopes (SS) while reducing the gate lengths from 10nm to 4nm. The gate length scaling with the 7nm diameter (D7) based NW delivers even worst electrostatics. The Fig. 5(c), compares SS variations for both the D7/D5 NW and the UFET transistor. In D5 NW, SS degradation from ~78mV/decade to ~160mV/decade is observed whereas, in UFET transistor, an SS degradation of ~87 mV/decade to ~112mV/decade is witnessed. At the applied potential, the distribution of electric fields inside the bulk UFET is shown in Fig. 6(a). The densely distributed fields along the channel dielectric would form a strong inversion channel inside the bulk while minimized field distribution in the low-k spacer would help to shrink the S/D to gate overlap parasitics. The impact of electrostatic potential spread by the buried gate is shown in Fig. 6(b). Also, the distribution of space charge is illustrated in Fig. 6(c). As the device operates

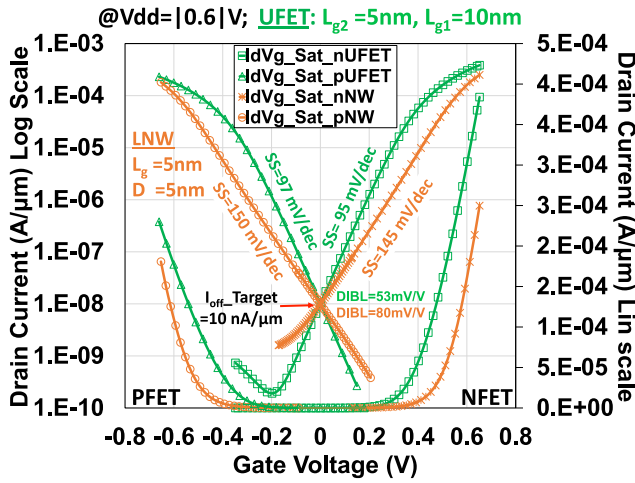


FIGURE 8. Saturation transfer characteristics compared for both the n-channel and the p-channel devices (UFET and GAA-NW FET).

TABLE 3. Electrostatics Comparison at the 5nm Foot-Print.

Parameters	D7 NW	D5 NW	UFET
SS_Sat (mV/decade)	185	150	95
DIBL (mV/V)	110	80	53

inside bulk silicon, one of the big challenges would be isolation between two devices. Fig. 6(d) shows the carrier distributions in multiple devices while isolated by the STI.

At the shortest gate length ($L_g = 5\text{nm}$ in NW, $L_{g2} = 5\text{nm}$ in UFET), distribution of (carrier) electron and electron current densities are shown in Fig. 7 during the ON ($V_g = 1\text{V}$, $V_{dd} = 0.6\text{V}$) and OFF ($V_g = 0\text{V}$, $V_{dd} = 0.6\text{V}$) state condition. At high and low applied gate voltages, the peak electron current densities of $8.343 \times 10^6 \text{A/cm}^2$ and $1.137 \times 10^2 \text{A/cm}^2$ are observed in the UFET device, whereas electron current densities of $2.229 \times 10^8 \text{A/cm}^2$ and $2.132 \times 10^5 \text{A/cm}^2$ are observed in D5 NW. This provides an on-off current ratio of 10^4 and 10^3 for UFET and NW respectively. The transfer ($I_d V_g$) characteristics (at $V_{dd} = 0.6\text{V}$) for both UFET and GAA-NW are plotted in Fig. 8. Compared to GAA-NW, the UFET shows $\sim 50\text{mV/decade}$ SS and $\sim 25\text{mV/V}$ DIBL improvements in both the n-channel and p-channel devices. The Table 3 summarizes SS and DIBL values for the GAA-NW and UFET.

In UFET, the buried gate-dielectric layer physically isolates the source and drain region, resulting in an effective shading between the drain electric field and the source electric field. This isolation at an ultra-scaled device would play a major role in conserving the short channel effects (such as SS, DIBL etc.). Also, the impact of direct S/D tunneling between source and drain is expected to be minimal, thus less leakage flow from source to drain is expected. The gate length scaling reduces L_{g2} part (foot-print gate length) of UFET's channel, continuing the area scaling, and maintaining larger physical channel length keeping the device capable of better off-state control.

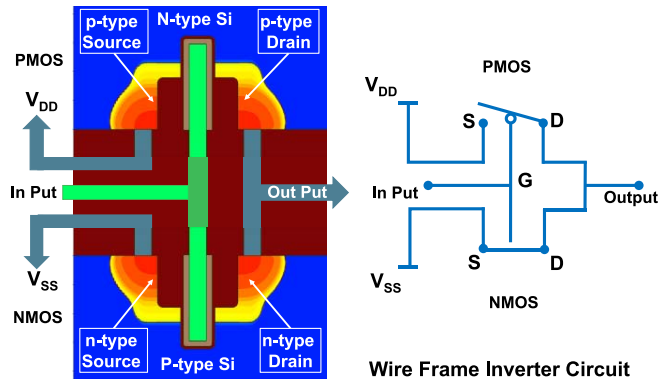


FIGURE 9. Proposal of Vertical Inverter shows the possibility of 50% area gain in scaling beyond the 3nm node.

IV. VERTICAL LOGIC CELL DESIGN

The novel UFET device has some key advantages over other device configuration such as: possibly easier process steps and scalability. The advantage of having a planar upper surface can be used to process another flipped UFET transistor to continue the scaling beyond 3nm node. Fig. 9 shows the schematic design of the proposed novel inverter. Vertically integrated top and the bottom device will be acting as a pull-up and pull-down devices which can be fabricated on a single transistor area (same on-wafer footprint). Source terminal of bottom n-channel UFET is connected to the lower potential (V_{ss}) and source terminal of top p-channel UFET is connected to the higher potential (V_{dd}). Both the gate and the drain terminals are continuously connected. The input is applied to the commonly connected gate and the output is taken from the commonly connected drain. This

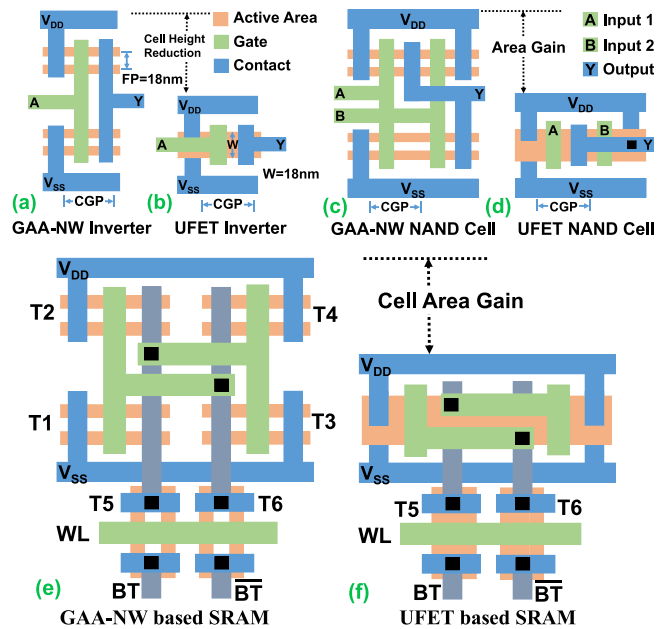


FIGURE 10. Layouts predicting an area gain while designing the vertical logic cell: (b) Basic Inverter, (d) NAND gate, and (f) SRAM cell.

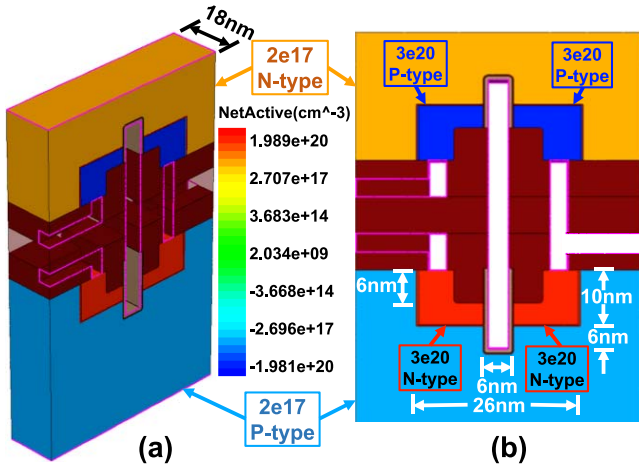


FIGURE 11. A simulated inverter: (a) Full 3D view, and (b) Cross-sectional 2D view showing all major device dimensions.

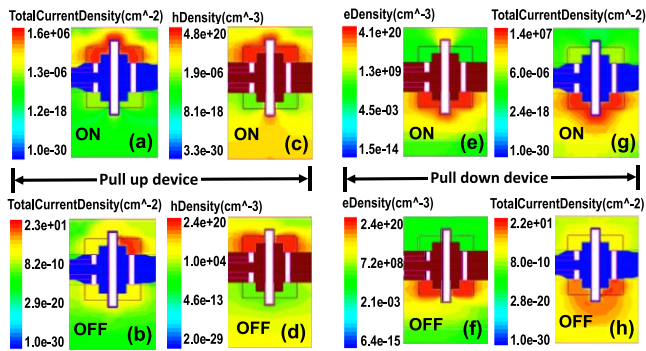


FIGURE 12. Simulated results showing distributions of majority carrier in both the pull up and the pull down devices at ON and OFF state condition.

approach will provide a significant area gain (Fig. 10(b)) especially for the beyond 5nm node when the footprint (L_g) scaling would be limited by the gate trench fill process. Continuing with this vertical design, the layout schematic in Fig. 10(d) and Fig. 10(f) shows cell height reduction in 4T NAND cell and in 6T SRAM cell. The layouts show in this paper are simplistic and area calculation will change considering the impact of contacts, isolation etc. on the actual layout design. Similar to this logic cell, other true logic gates such as transmission gate and pass gate can also be designed.

Current development of monolithic 3D integration has enabled a new direction of CMOS integration. The vertical stacking [25]–[27] along with many technological breakthroughs in TSV [28] and ultra-thin FDSOI [29], [30] process, would help to accomplish the proposed UFET based vertical integration. Novel vertical design with two transistor inverter is simulated using the Sentaurus-Device. Specifying all the major dimensions, the 3D schematic inverter is shown in Fig. 11. The footprint gate length of 6nm and trench depth of 16nm is considered, in where the CGP is scaled down to less than 24nm.

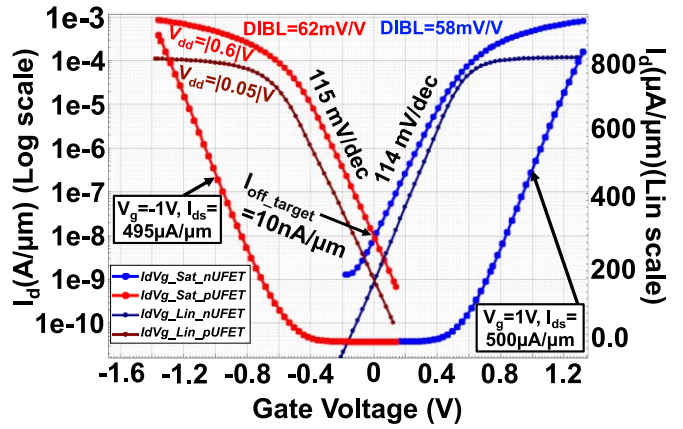


FIGURE 13. The transfer characteristics ($I_d V_g$) for both the pull-up and pull down UFET.

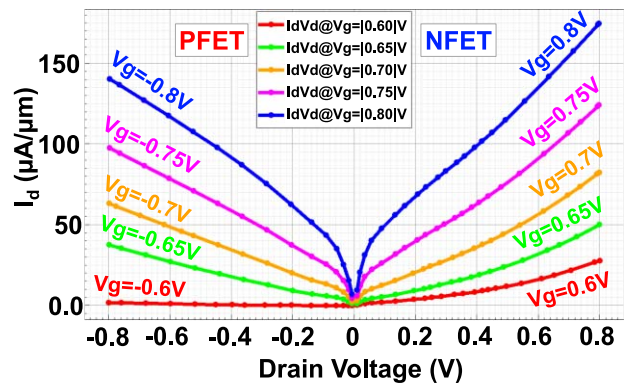


FIGURE 14. Output characteristics ($I_d V_d$) for both the n-channel and p-channel UFET.

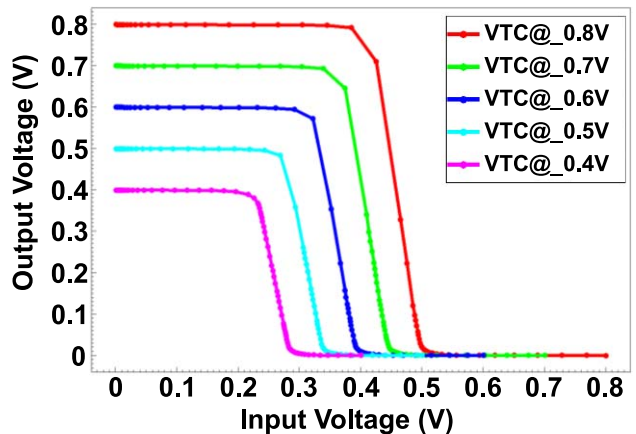


FIGURE 15. The voltage transfer characteristics (VTC) of proposed vertical inverter at different drive voltages.

While analyzing the electrical behavior of this compact inverter, the distributions of majority carriers during ON and OFF state condition are shown in Fig. 12. Although the applied potential at continuously connected gate terminal may influence the opposite device, the lower potential at source/drain will mitigate the impact, similar to the

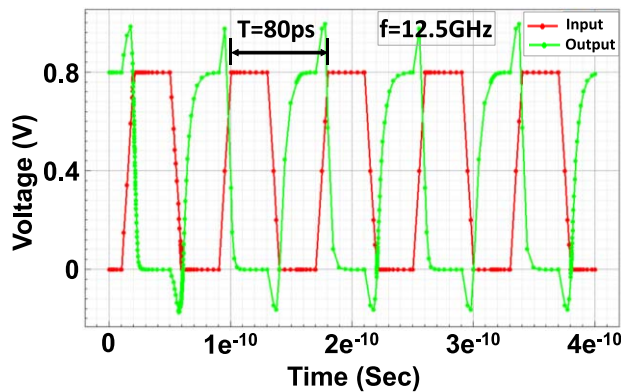


FIGURE 16. Transient behavior of the vertical inverter with a pulsed input signal.

planar MOSFET based circuit design. The transfer ($I_d V_g$) and output ($I_d V_d$) characteristics for both the pull-up and pull-down devices are plotted in Fig. 13 and in Fig. 14. Smooth transition of voltage transfer characteristics (VTC) for the inverter operation even at a lower operating voltage of 0.4V is shown in Fig. 15. Along with a sharper VTC, the transient output (Fig. 16) predicts a proper inverter circuit.

In order to investigate the full AC behavior of this device, detailed studies are required. The proposed novel device can be a potential candidate for scaling the 3nm node and beyond CMOS transistors. At current situation, there is a very limited space to scale down the device size further in lateral direction, hence this vertical integration enables a novel trend of CMOS scaling for the next generation technology.

V. CONCLUSION

An alternative device architecture has been presented in this paper for the future trend of CMOS scaling. Using a recessed channel UFET architecture, the CGP can be scaled down to 24nm, leading to a transistor where scaling in size and lowering the leakage might be achieved together. The advantage of having a flat surface in UFET enables the vertical integration of an inverter. Finally, the vertical logic gate has the possibility of achieving significant (~50%) area gain for ultimate scaling of CMOS technology.

REFERENCES

- [1] G. E. Moore, "Cramming more components onto integrated circuits," *Electronics*, vol. 38, no. 8, pp. 114–117, Apr. 1965.
- [2] K. Mistry *et al.*, "Delaying forever: Uniaxial strained silicon transistors in a 90nm CMOS technology," in *Proc. IEEE VLSI Technol. Symp.*, Honolulu, HI, USA, Jun. 2004, pp. 50–51, doi: [10.1109/VLSIT.2004.1345387](https://doi.org/10.1109/VLSIT.2004.1345387).
- [3] C. Auth *et al.*, "45nm high-k + metal gate strain-enhanced transistors," in *Proc. IEEE VLSI Technol. Symp.*, Honolulu, HI, USA, Jun. 2008, pp. 128–129, doi: [10.1109/VLSIT.2008.4588589](https://doi.org/10.1109/VLSIT.2008.4588589).
- [4] S. Natarajan *et al.*, "A 32nm logic technology featuring 2nd-generation high-k + metal-gate transistors, enhanced channel strain and 0.171 μm^2 SRAM cell size in a 291Mb array," in *Proc. IEEE Int. Electron Devices Meeting*, San Francisco, CA, USA, Dec. 2008, pp. 1–3, doi: [10.1109/IEDM.2008.4796777](https://doi.org/10.1109/IEDM.2008.4796777).

- [5] C. Auth *et al.*, "A 22nm high performance and low-power CMOS technology featuring fully-depleted tri-gate transistors, self-aligned contacts and high density MIM capacitors," in *Proc. IEEE VLSI Technol. Symp.*, Honolulu, HI, USA, Jun. 2012, pp. 131–132, doi: [10.1109/VLSIT.2012.6242496](https://doi.org/10.1109/VLSIT.2012.6242496).
- [6] S.-Y. Wu *et al.*, "An enhanced 16nm CMOS technology featuring 2nd generation FinFET transistors and advanced Cu/low-k interconnect for low power and high performance applications," in *Proc. IEEE Electron Devices Meeting*, San Francisco, CA, USA, Dec. 2014, pp. 1–3, doi: [10.1109/IEDM.2014.7046970](https://doi.org/10.1109/IEDM.2014.7046970).
- [7] S. Natarajan *et al.*, "A 14nm logic technology featuring 2nd-generation FinFET, air-gapped interconnects, self-aligned double patterning and a 0.0588 μm^2 SRAM cell size," in *Proc. IEEE Electron Devices Meeting*, San Francisco, CA, USA, Dec. 2014, pp. 3–7, doi: [10.1109/IEDM.2014.7046976](https://doi.org/10.1109/IEDM.2014.7046976).
- [8] C. Auth *et al.*, "A 10nm high performance and low-power CMOS technology featuring 3rd generation FinFET transistors, self-aligned quad patterning, contact over active gate and cobalt local interconnects," in *Proc. IEEE Electron Devices Meeting*, San Francisco, CA, USA, Dec. 2017, pp. 1–29, doi: [10.1109/IEDM.2017.8268472](https://doi.org/10.1109/IEDM.2017.8268472).
- [9] H.-J. Cho *et al.*, "Si FinFET based 10nm technology with multi Vt gate stack for low power and high performance applications," in *Proc. IEEE VLSI Technol. Symp.*, Honolulu, HI, USA, Jun. 2016, pp. 1–2, doi: [10.1109/VLSIT.2016.7573359](https://doi.org/10.1109/VLSIT.2016.7573359).
- [10] R. Xie *et al.*, "A 7nm FinFET technology featuring EUV patterning and dual strained high mobility channels," in *Proc. IEEE Electron Devices Meeting*, San Francisco, CA, USA, Dec. 2016, pp. 2–7, doi: [10.1109/IEDM.2016.7838334](https://doi.org/10.1109/IEDM.2016.7838334).
- [11] S. Narasimha *et al.*, "A 7nm CMOS technology platform for mobile and high performance compute application," in *Proc. IEEE Electron Devices Meeting*, Dec. 2017, pp. 29.5.1–29.5.4, doi: [10.1109/IEDM.2017.8268476](https://doi.org/10.1109/IEDM.2017.8268476).
- [12] S. D. Kim *et al.*, "Performance trade-offs in FinFET and gate-all-around device architectures for 7nm-node and beyond," in *Proc. IEEE SOI-3D Subthreshold Microelectron. Technol. Unified Conf.*, Oct. 2015, pp. 1–3, doi: [10.1109/S3S.2015.7333521](https://doi.org/10.1109/S3S.2015.7333521).
- [13] N. Loubet *et al.*, "Stacked nanosheet gate-all-around transistor to enable scaling beyond FinFET," in *Proc. IEEE VLSI Technol. Symp.*, Jun. 2017, pp. T230–T231, doi: [10.23919/VLSIT.2017.7998183](https://doi.org/10.23919/VLSIT.2017.7998183).
- [14] R. Divakaruni and V. Narayanan, "(Keynote) challenges of 10 nm and 7 nm CMOS for server and mobile applications," *ECS Trans.*, vol. 72, no. 4, pp. 3–14, May 2016, doi: [10.1149/07204.0003ecst](https://doi.org/10.1149/07204.0003ecst).
- [15] U. K. Das *et al.*, "Limitations on lateral nanowire scaling beyond 7-nm node," *IEEE Electron Device Lett.*, vol. 38, no. 1, pp. 9–11, Jan. 2017, doi: [10.1109/LED.2016.2629420](https://doi.org/10.1109/LED.2016.2629420).
- [16] J. Tanaka *et al.*, "Simulation of sub-0.1- μm MOSFETs with completely suppressed short-channel effect," *IEEE Electron Device Lett.*, vol. 14, no. 8, pp. 396–399, Aug. 1993, doi: [10.1109/55.225591](https://doi.org/10.1109/55.225591).
- [17] J. Y. Kim *et al.*, "The breakthrough in data retention time of DRAM using recess-channel-array transistor (RCAT) for 88 nm feature size and beyond," in *Proc. IEEE VLSI Technol. Symp.*, Jun. 2003, pp. 11–12, doi: [10.1109/VLSIT.2003.1221061](https://doi.org/10.1109/VLSIT.2003.1221061).
- [18] S.-W. Chung *et al.*, "Highly scalable saddle-fin (S-Fin) transistor for sub-50nm DRAM technology," in *Proc. VLSI Technol. Symp.*, Honolulu, HI, USA, Jun. 2006, pp. 32–33, doi: [10.1109/VLSIT.2006.1705202](https://doi.org/10.1109/VLSIT.2006.1705202).
- [19] R. A. Wickstrom, "VMOS transistor," U.S. Patent 4070690, Jan. 24, 1978.
- [20] *Sentaurus™ Process User Guide, L-2016.12*, Synopsys, Mountain View, CA, USA, 2016.
- [21] *Sentaurus™ Device User Guide, L-2016.12*, Synopsys, Mountain View, CA, USA, 2016.
- [22] B. Turkot and S. Carson, and A. Lio, "Continuing Moore's law with EUV lithography," in *Proc. IEEE Electron Devices Meeting (IEDM)*, San Francisco, CA, USA, Dec. 2017, pp. 14.4.1–14.4.3, doi: [10.1109/IEDM.2017.8268390](https://doi.org/10.1109/IEDM.2017.8268390).
- [23] Sentaurus™ Project Demonstrates, *Three-Dimensional Simulation of 14/16 nm FinFETs With Round Fin Corners and Tapered Fin Shape, Version H-2013.03*, Synopsys, Mountain View, CA, USA, 2013.
- [24] S. Datta, *Electronic Transport in Mesoscopic Systems*. Cambridge, U.K.: Cambridge Univ. Press, 1997.
- [25] S. Wong *et al.*, "Monolithic 3D integrated circuits," in *Proc. IEEE VLSI Technol. Syst. Appl. Symp.*, Apr. 2007, pp. 1–4, doi: [10.1109/VTSA.2007.378923](https://doi.org/10.1109/VTSA.2007.378923).

- [26] T. Naito *et al.*, "World's first monolithic 3D-FPGA with TFT SRAM over 90nm 9 layer Cu CMOS," in *Proc. IEEE VLSI Technol. Symp.*, Jun. 2010, pp. 219–220, doi: [10.1109/VLSIT.2010.5556234](https://doi.org/10.1109/VLSIT.2010.5556234).
- [27] J. Shi *et al.*, "A 14nm FinFET transistor-level 3D partitioning design to enable high-performance and low-cost monolithic 3D IC," in *Proc. IEEE Electron Devices Meeting*, San Francisco, CA, USA, Dec. 2016, pp. 2–5, doi: [10.1109/IEDM.2016.7838032](https://doi.org/10.1109/IEDM.2016.7838032).
- [28] L. England and I. Arsovski, "Advanced packaging saves the day!—How TSV technology will enable continued scaling," in *Proc. IEEE Electron Devices Meeting*, San Francisco, CA, USA, Dec. 2017, pp. 3.5.1–3.5.4, doi: [10.1109/IEDM.2017.8268320](https://doi.org/10.1109/IEDM.2017.8268320).
- [29] K. Cheng *et al.*, "High performance extremely thin SOI (ETSOI) hybrid CMOS with Si channel NFET and strained SiGe channel PFET," in *Proc. IEEE Electron Devices Meeting*, San Francisco, CA, USA, Dec. 2012, pp. 18.1.1–18.1.4, doi: [10.1109/IEDM.2012.6479063](https://doi.org/10.1109/IEDM.2012.6479063).
- [30] K. Cheng, B. B. Doris, A. Khakifirooz, and D. C. La Tulipe, Jr., "Semiconductor device with a low-K spacer and method of forming the same," U.S. Patent 9583628, Feb. 28, 2017.



UTTAM KUMAR DAS received the B.Tech. degree in electronics and communication engineering from Jalpaiguri Government Engineering College, Jalpaiguri, India, in 2012 and the M.Tech. degree in VLSI and microsystems from the Indian Institute of Space Science and Technology, Trivandrum, India, in 2015. He was with the Design-Enabled Technology Exploration team at imec, Leuven, Belgium, in 2016. He is currently with the Department of Electronics and Electrical Communication Engineering, Indian Institute of

Technology Kharagpur, Kharagpur, India. He is working on various logic device for the advance node CMOS application. His research interests are emerging device architectures, simulation, modeling and their fabrication.



GEERT ENEMAN received the B.S. and M.S. degrees in electrical engineering and the Ph.D. degree on the topic of "Design, fabrication, and characterization of strained silicon transistors" from the Katholieke Universiteit Leuven, Leuven, Belgium, in 1999, 2002, and 2006, respectively. His Ph.D. work was done at the IMEC Leuven. He has been with imec since 2011. His current research interests include characterization of Ge and III-V MOSFETs, and modeling of alternative device structures.



RAVI SHANKAR R. VELAMPATI received the Ph.D. degree in electrical engineering from the University of Connecticut, Storrs, CT, USA, in 2007. His Ph.D. thesis focused on fabrication, characterization, and modeling of quantum dot gate nonvolatile memory devices. After his doctoral work, he was a Process Technology Development Engineer with Intel Corporation's Technology Development wing, where he was involved in the development of dielectrics to enable scaling down of NOR Flash Memory

Devices and logic CMOS devices in 65, 45, and 32 nm technology nodes. He relocated to India to work on development and technology transfer of 180-nm CMOS technology from TowerJazz Ltd., Israel, to Semiconductor Laboratory (SCL), Department of Space, Govt. of India. After a brief stint in academia as a faculty in the Indian Institute of Space Science and Technology and the Indian Institute of Technology Ropar. He is currently a Scientist with VLSI Fabrication Division, Semiconductor Laboratory, Department of Space, Govt. of India.



YOGESH SINGH CHAUHAN (SM'12) is an Associate Professor with the Indian Institute of Technology Kanpur, India. He was with Semiconductor Research and Development Center, IBM Bangalore from 2007 to 2010, the Tokyo Institute of Technology in 2010, the University of California Berkeley from 2010 to 2012, and ST Microelectronics from 2003 to 2004. He is the developer of industry standard BSIM-BULK (formerly, BSIM6) model for bulk MOSFETs and ASM-HEMT model for GaN HEMTs. His group

is also involved in developing compact models for FinFET, nanosheet/gate-all-around FET, FDSOI transistors, negative capacitance FETs, and 2-D FETs.

He is the Editor of the IEEE TRANSACTIONS ON ELECTRON DEVICES and a Distinguished Lecturer of the IEEE Electron Devices Society. He is the member of IEEE-EDS Compact Modeling Committee and a fellow of the Indian National Young Academy of Science. He is the Founding Chairperson of IEEE Electron Devices Society U.P. chapter and the Vice-Chairperson of IEEE U.P. section. He has published over 200 papers in international journals and conferences.

Dr. Chauhan was a recipient of the Ramanujan Fellowship in 2012, the IBM Faculty Award in 2013 and P. K. Kelkar Fellowship in 2015, and the CNR Rao Faculty Award and Humboldt Fellowship in 2018. His research interests are characterization, modeling, and simulation of semiconductor devices. He has served in the technical program committees of IEEE International Electron Devices Meeting, IEEE International Conference on Simulation of Semiconductor Processes and Devices, IEEE European Solid-State Device Research Conference, IEEE Electron Devices Technology and Manufacturing, and IEEE International Conference on VLSI Design and International Conference on Embedded Systems.



K. B. JINESH received the M.S. degree in physics from the Cochin University of Science and Technology, India, in 2000 and the Ph.D. degree in physics from Leiden University, The Netherlands, in 2006. He was a Researcher with the Jawaharlal Nehru Center for Advanced Scientific Research, India, in 2001 and the Delft University of Technology, The Netherlands, in 2002. From 2006 to 2008, he was a Scientist with NXP Semiconductors, working in the field of atomic layer deposited high-k materials, especially, binary and ternary rare-earth metal oxides for high-density capacitor applications.

He was with IMEC Netherlands as a Researcher working in the field of sensors and actuators in 2009. He is currently an Associate Professor with IIST Trivandrum, India. His current research interests include the charge transport mechanisms through nanostructures, scaling advanced CMOS devices and future memory technology.



TARUN K. BHATTACHARYYA received the M.E. and Ph.D. degrees in electronics and telecommunication engineering from Jadavpur University, Kolkata, in 1991 and 1996, respectively. He has served as a Scientist in areas of thin film and micro-electronics technology in many reputed laboratories, such as Indian Association for Cultivation of Science, Central Glass and Ceramic research Institute, Kolkata, and the University of Kaiserslautern, Germany. He has been a Visiting Faculty Member with the University of

Washington and the University of Michigan. Since 2000, he has been a Professor with the Electronics and Electrical Communication Engineering Department, Indian Institute of Technology Khargapur, Khargapur, India. He was a recipient of the UNIDO (Vienna) Fellowship in 1992 and the IBM Faculty Award for the year 2012. He served as a Technical Committee Member of VLSI Design Conference in 2007. He is a member of Indo-Japan collaborative committee on Advanced Micro-Nano Manufacturing Science. He is also a member of Indo-U.S. Frontiers of Engineers.